

Available online at www.jonass.ir

Journal of Nature and Spatial Sciences

Journal homepage: www.jonass.ir

Original Article



GIS-based support vector machine model in shallow landslide hazards prediction: A case study on Ilam dam watershed, Iran

Yaghoub Niazi^{a*}, Manuel E. Mendoza^b, Ali Talebi^c and Hasti Bidaki^c

^a MAGTA Development Center Company, Ilam, Iran

^b Centro de Investigaciones en Geografía Ambiental, Universidad Nacional Autónoma de México, Mexico

^c Faculty of Natural Resources, Yazd University, Yazd, Iran

ARTICLE INFO

Article history:

Received 09 February 2021

Revised 03 March 2021

Accepted 03 March 2021

Published online Apr 2021

Keywords:

Landslide susceptibility mapping;

Support vector machines (SVM);

GIS;

Ilam dam

ABSTRACT

Background and objective: The SVM algorithm is an applied method that has been considered in recent years to study landslides. The main purpose of this study is to evaluate the mapping power of the GIS-based SVM model with kernel functions analysis for spatial prediction of landslides at the Ilam dam watershed.

Materials and methods: According to review sources, 14 underlying factors including elevation, slope, aspect, plan curvature, profile curvature, LS factor, TWI, SPI, lithological units, land cover, NDVI, road distance, distance to the drainage channel, distance to fault were selected as factors affecting the occurrence of landslides in the study area and the mentioned layers were prepared in the GIS. In the present study, the non-linear two-class SVM method was used, the two-class SVM requires both datasets representing the occurrence of landslides and non-occurrence of landslides. The landslide inventory was randomly divided into a training dataset of 75% for building the models and the remaining 25% for the validation of the models.

Results and conclusion: The validation results showed that the area of the prediction-rate curve under the curve (AUC) for landslide susceptibility maps produced by the SVM linear function, SVM polynomial function, SVM radial basic function, and SVM sigmoid function are 0.946, 0.931, 0.912, and 0.871 respectively. To assess the influences of factors on the landslide susceptibility map were used the Cohen's kappa index of the model. The result shows that the most effective factors are the distance to roads, distance to drainages, and plan curvature in this area.

1. Introduction

Natural events are complex processes that affect all parts of the planet. In this context, landslides, as one of the natural hazards, are always occurring all over the world and are of great importance. Landslides represent the most damaging natural hazards in the mountainous areas of different parts of the world, causing loss of human life, property damage, and consequently economic crisis. These

* Corresponding author. Tel.: +98-918-344-7941.

E-mail address: niazi.yb@gmail.com, ORCID: 0000-0001-5174-1886

Peer review under responsibility of Maybod Branch, Islamic Azad University

2783-1604/© 2021 Published by Maybod Branch, Islamic Azad University. This is an open access article under the CC BY license

(<http://creativecommons.org/licenses/by/4.0/>)

DOI: [10.30495/jonass.2021.680329](https://doi.org/10.30495/jonass.2021.680329)

landslides are caused by various external factors such as natural factors such as earthquakes, volcanoes, and human activities. (Lin et al., 2008; Hadi et al., 2018; Gordo et al., 2019). According to the Center for Disaster Epidemiology Research (CRED), landslides are responsible for at least 17% of natural disaster losses worldwide. On a global scale, landslides cause billions of dollars in damage and thousands of deaths and injuries each year. Developing countries suffer the most, where 0.5% of gross domestic product (GDP) per year is lost due to landslides and 95% of landslides are recorded in developing countries (Chung et al., 1995). This trend is expected to continue in the future due to increased unplanned urbanization and development, continued deforestation, and increased regional precipitation as a result of changing climatic conditions in landslide-prone areas (Kanungo et al., 2009; Goetz et al., 2011). At the end of September 2007, About 187 people have been killed by landslides, and losses resulting from mass movements having been estimated at almost 12,700 million dollars using the 4900 landslide database In Iran (Iranian landslide working party, 2007). Due to the importance of cognition, risk factors are necessary for zoning landslide hazards (Iranian landslide working party, 2007).

To solve these problems, landslide susceptibility maps can play an important role in determining areas vulnerable to landslides. Landslide susceptibility map preparation is considered the first important step for landslide hazard mitigation and management. Over the decades, the topic of landslide susceptibility mapping has been discussed and investigated by many researchers (Yılmaz, 2009; Dai et al., 2001; Yao et al., 2008; Bednarik et al., 2012). In recent years, the use of GIS for landslide risk modeling has increased due to the rapid and high-precision access to data obtained through Global Positioning Systems (GPS) and remote sensing (e.g., Saha et al., 2005; Pradhan et al., 2011, 2013; Bednarik et al., 2012; Mohammady et al., 2012; Devkota et al., 2013; Pourghasemi et al., 2013a, 2013b, 2019; Gordo et al., 2019; Roccati et al., 2019; Yan et al., 2019). Moreover, GIS is an excellent and useful tool for the spatial analysis of a multi-dimensional phenomenon, such as landslides and landslide susceptibility mapping (Van Westen et al., 1990). Over the last decades, many different methods for landslide susceptibility mapping have been used and suggested. Many studies have been carried out on landslide hazard evaluation using GIS (Guzzetti et al., 1999). Landslide susceptibility has been illustrated in versatile techniques in various case studies, yielding more or less reliable results, depending on the complexity of the terrain and the suitability of the approach (Bonham-Carter, 2002). All those attempts came to a common conclusion; that the problem dealt with in the scope of landslide assessment tends to be non-linear, due to the complexity of the geological environment, as well as triggering factors (storms, earthquakes, erosion, human influence, etc.) (Brenning, 2005).

Over the last decade, different models were used for landslide susceptibility mapping such as probabilistic models (Gokceoglu and Aksoy, 1996; Talebi et al., 2008b; Akgun and Turk 2010; Budimir et al. 2015; Pradhan 2011; Pradhan and Lee 2010; Pourghasemi et al., 2018), logistic regression, one of the most widely used statistical models, has also been employed for landslide susceptibility mapping (Guzzetti et al., 1999; Yılmaz, 2009; Wang et al., 2013; Budimir et al., 2015; Reichenbach et al., 2018), and geotechnical and the safety factor models (Talebi et al., 2008a). Recently, other new methods have been applied for landslide susceptibility evaluation using soft computing and data mining approaches such as fuzzy logic (Ilanloo 2011; Pourghasemi et al., 2012a; Gheshlaghi and Feizizadeh, 2017), artificial neural network models (Lee et al., 2003; Ermini et al., 2005; Zare et al., 2013; Aditian et al., 2018), neuro-fuzzy (Oh & Pradhan, 2011; Chen et al., 2017), decision tree methods (Yeon et al., 2010; Hong et al., 2018), spatial multi criteria evaluation (Pourghasemi et al., 2012b; Günther et al., 2014; Pradhan and Kim, 2016), evidential belief function model (Althuwaynee et al. 2012; Lee et al. 2013), Dempster–Shafer and weights-of-evidence models (Tangestani, 2001 Dahal et al., 2008), support vector machine (SVM) (Bui et al., 2012a, 2012b; Hong et al., 2015; Colkesen et al., 2016; Lee et al., 2017; Chen et al., 2017; Kalantar et al., 2018; Pourghasemi and Rahmati, 2018; Huang and Zho, 2018; Pourghasemi et al., 2020) and their performances have been assessed. Among these approaches, SVM modeling, which is a method based on statistical learning theory and involves a training phase related to the target input and output values, has become increasingly popular. (Yao et al., 2008). The damage from rainfall-induced landslides in the Ilam dam watershed can be partly attributed to both the lack of landslide assessment and prediction, and the lack of response plans for minimizing the impacts of the landslides. Therefore, it is imperative to enhance the capability to detect and predict geological hazards

like landslides and to prevent or reduce the risk to life, property, social and economic activities, and natural resources.

The main aim of the present study is to produce a landslide susceptibility map using a GIS-based support vector machine model. Because SVM is a high-performing machine learning algorithm, different kernel functions of SVM were applied and validated in the Ilam dam watershed. Scientifically, the comparison of various kernel classifiers is important because SVM can use several types of kernel functions. Also, the effect of each factor in the sensitivity analysis was evaluated by validation of landslide susceptibility maps. This study may contribute to the selection of kernel function and impact factors for the landslide susceptibility mapping by the SVM approach.

2. Study area

The study area is called the Ilam dam watershed, located in the southeast of Ilam Province in western Iran. The study area is called the Ilam dam watershed, located in the southeast of Ilam Province in western Iran. The watershed area is 476.7 km² and lies between 33°23' 32" to 33°38' 51" north latitudes and 46°20' 30" to 46°39' 33" east longitudes (Fig. 1). The elevations at the highest and lowest points are 2600 m and 900 m above mean sea level, respectively. Climatic conditions in the area are semi-arid (typical Mediterranean climate) with 595 mm rainfall, and the average temperature is 21.7°C in summer and 4.7°C in winter. Land cover in the area mostly includes agricultural land, barren land, forest land, grassland, garden land, and water body. The Ilam dam is one of the most important dams in western Iran that supplies drinking water to the Ilam city.

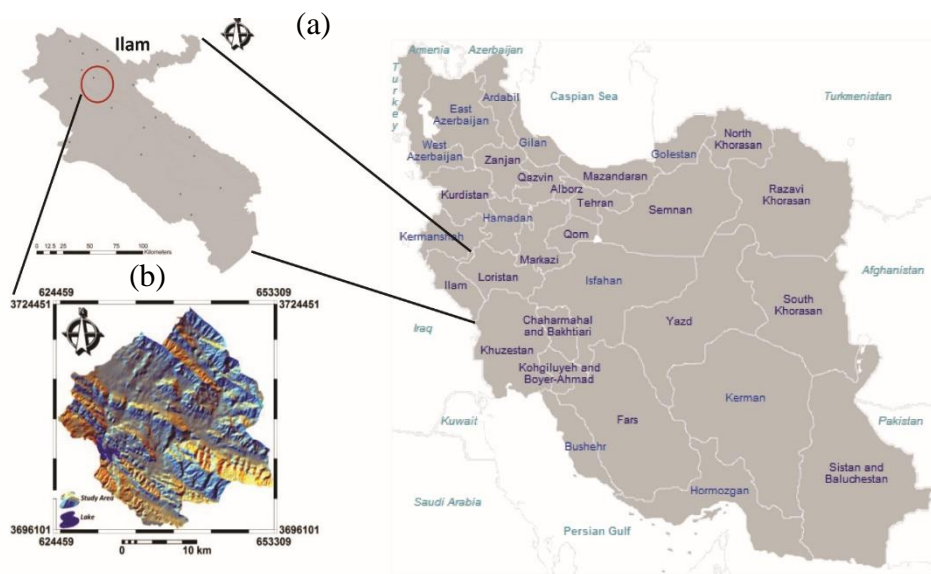


Fig. 1- Study area. a) Location of Ilam Province in Iran, b) hill-shade of the study area.

3. Data used

3.1. Landslide inventory map

Implementing a landslide susceptibility model needs a clear understanding of the relationship between the landslide inventory dataset and the landslide conditioning factors (Ercanoglu and Gokceoglu, 2003; van Westen et al., 2006; Petley, 2008). Accurate detection of landslide location and creating the historical database record are very important for landslide susceptibility analysis. Remote sensing methods, using aerial photographs and satellite images as well as extensive field surveys and

observations, were used to produce a detailed and reliable landslide inventory map, in the study area. A total of 45 landslides were identified and mapped in the study area by evaluating aerial photos on a 1:25,000 scale supported by a field survey (Fig. 2). Most of the landslides are shallow rotational with a few translational that occurred in cut-slopes or embankments, alongside roads, highways in the mountainous regions of the study area. All the 45 landslides that were included in the study occurred over the past 20 years (1993-2013). In this study, 90 absence and presence data of landslides were identified, 75% locations were chosen randomly for the landslide susceptibility modeling, while the remaining 25% cases were used for the model validation.

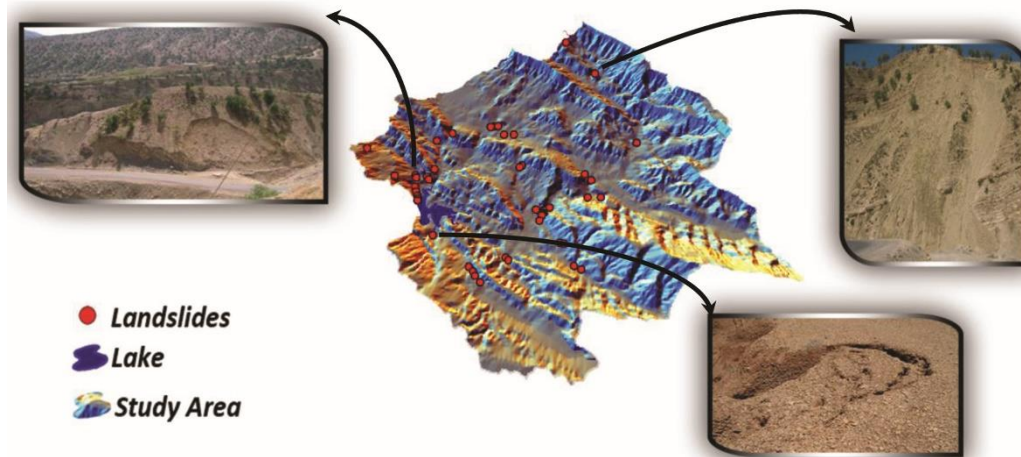


Fig. 2- Landslide inventory map (special distribution of landslides in the study area).

3.2. Landslide conditioning factors

To achieve high accuracy of the landslide susceptibility model in predicting landslide vulnerable areas, selecting and preparing the landslide conditioning factors database is a vitally important step. The landslide conditioning factors in the current study were selected based on the information collected from the literature, related to the study area, and field investigation (Pourghasemi et al., 2013a, b, c; Tseng et al., 2015; Bui et al., 2016; Kornejady et al., 2017; Ghorbanzadeh et al., 2019; Xiao et al., 2019). Tseng et al. (2015) noted that the choice of landslide-related factors (known as internal factors) depends on the characteristics of the study area, the landslide type, and the scale of the analysis. There were a total of fourteen landslide conditioning factors considered in the analyses performed. The basic landslide conditioning factors such as elevation, slope gradient, slope aspect, slope length, topographic wetness index (TWI), Stream Power Index (SPI), plan curvature, profile curvature, distance from drainage, surface material and, distance to fault, land cover, distance to road and NDVI were employed. Thematic layers were acquired from different resources using ArcGIS, SAGA, ILWIS, and ENVI packages. The descriptions of the used input data, their spatial resolution, and the sources are given in Table 1 and briefly explained below. As mentioned in this table the resolution of all conditioning factors is 15 m because we used ASTER satellite imagery (15-m resolution) to produce several base maps (Fig. 3).

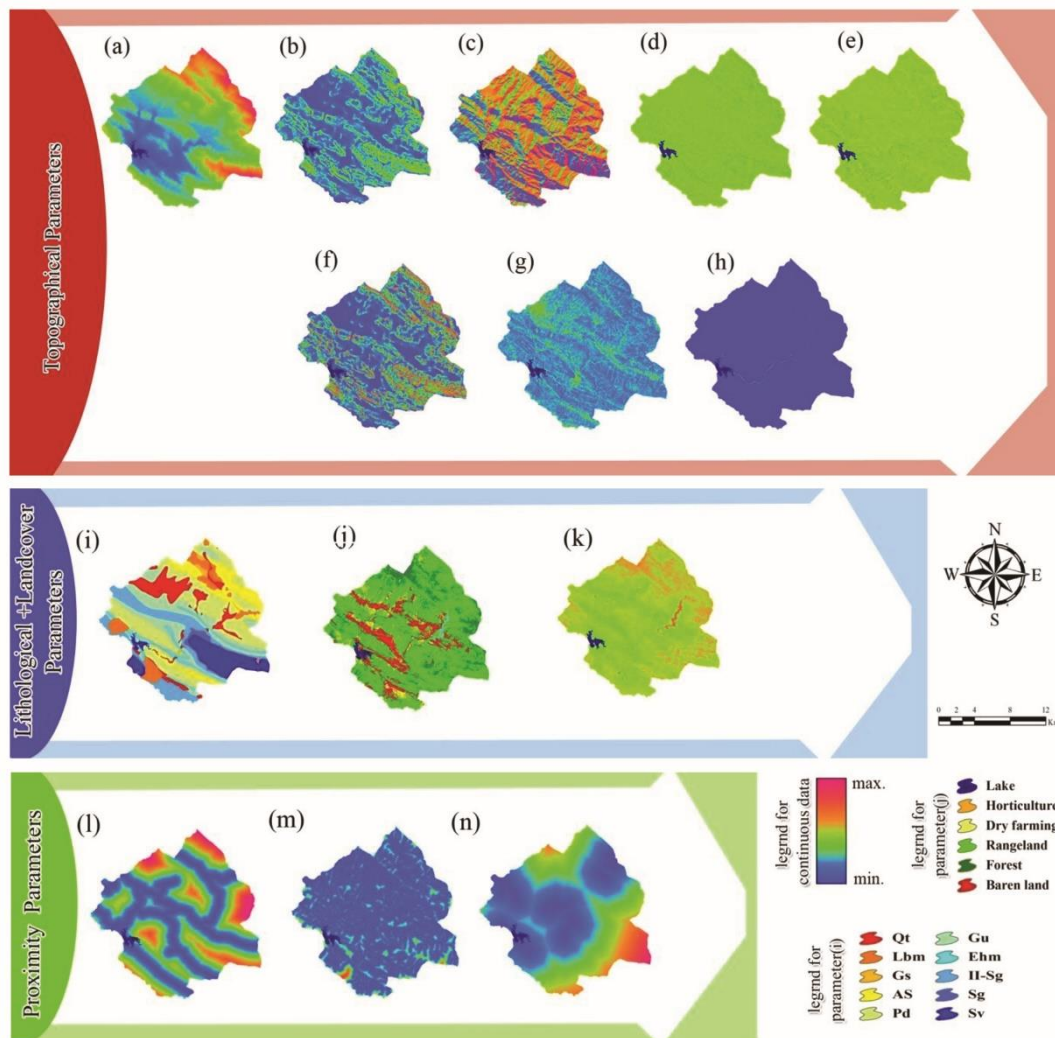


Fig. 3- Input parameters (landslide triggering factors) in the study area. a) elevation, b) slope, c) aspect, d) plan curvature, e) profile curvature, f) LS factor, g) TWI, h) SPI, i) Lithologic units, j) land cover, k) NDVI, l) road distance, m) distance to the drainage channel, n) distance to the fault.

Table 1- Raster thematic maps of the input dataset.

Spatial data attributes (notation)	Source, scale/resolution	Short description
Elevation	ASTER image, 15 m	DEM of the terrain surface
Slope	DEM, 15 m	The angle of the slope inclination
Aspect	DEM, 15 m	Exposition of the slope
Slope length	DEM, 15 m	Length factor of the slope
Topographic wetness index	DEM, 15 m	The ratio of the contributing area a and tg (slope)
Stream power index	DEM, 15 m	Multiplication of contributing area a and tg (slope)
Plan curvature	DEM, 15 m	Index of concavity parallel to the slope
Profile curvature	DEM, 15 m	Index of concavity perpendicular to the slope
Distance from the stream	DEM, 15 m	A buffer of the drainage network
Lithology	Geo-map, 1:100,000- ASTER image, 15 m	Surface material units
Distance from fault	Geo-map, 1:100,000- ASTER image, 15 m	Buffer of structure
Distance from the road	Topo- map , 1:25,000- ASTER image, 15 m	Buffer of road
Landuse/landcover	ASTER image, 15 m	Image classification using artificial neural network (ANN) algorithm
NDVI	ASTER image, 15 m	Interpretation of vegetation, water bodies, and bare soil, based on NDVI

3.2.1. Elevation

Some researchers use elevation as a controlling parameter for landslides (Dai et al., 2001; Yilmaz, 2010). It is well known that elevation influences many biophysical parameters and anthropogenic activities. These parameters and activities are likely to affect slope stability and generate slope failure. Elevation affects soil characteristics such as soil (regolith) depth (Kuriakose et al., 2009b) and soil mechanical and hydrological properties, which in turn affects slope stability (van Beek and van Asch, 2004). In this study, an altitude map was prepared according to the classification of the built DEM (Fig. 3a).

3.2.2. Slope gradient

The most important parameter in the slope stability analysis is the slope gradient (Lee and Min 2001). Because the slope gradient is directly related to the landslides and it is frequently used in preparing landslide susceptibility maps (Clerici et al. 2002; Saha et al., 2005; Cevik and Topal 2003; Ercanoglu and Gokceoglu, 2003; Lee and Talib, 2005). The slope gradient is defined by Burrough (1986) as the maximum rate of change in altitude. Hill-slope material (in the form of debris or rock) can move downslope in response to gravity. Movement can range from very slow, barely perceptible over many years, to devastatingly rapid, within seconds. Shrestha and Zinck (2001), Ercanoglu, and Gokceoglu (2003) argue that slope gradient can be considered the most important landslide conditioning factor. Slope gradient determines the convergence and divergence of water on a hill-slope and thereby influences soil water content and slope stability. It has been widely shown that landslides tend to occur more frequently on steeper slopes (Vijith and Madhu, 2008; McDermid and Franklin, 1995; Cooke and Doornkamp, 1990). Bui et al. (2017) concluded that slope gradient is related both to the shear stresses acting on the hill slope and to the displacement of the landslide mass. The slope angle map of the current study was derived from the Digital Elevation Model (DEM) with a resolution of 15 m, (Fig. 3b).

3.2.3. Slope Aspect

Slope aspect is defined as the compass direction of the maximum rate of change and is considered by some researchers as a landslide conditioning factor (Van Westen and Bonilla 1990; Gokceoglu and Aksoy, 1996; Saha et al., 2005; Ercanoglu and Gokceoglu, 2003; Devkota et al., 2013). In mountainous areas, the direction of the slopes (aspect) is such that some slope faces the direct rays of the sun while others receive indirect sunlight (Guzetti et al., 1999). They continue to state that this may also influence the vegetation condition, which is often different for various aspect classes. Also because of their relative exposure, some slopes experience more rain than others and this influences the local soil mechanical and hydrological conditions. Although some authors (e.g. Greenbaum et al., 1995) have found that aspect has no significant influence on a landslide, several researchers have reported a relationship between slope aspect and landslide occurrence. For example, according to a report by Lineback et al. (2001),

more landslides occur in the wetter northern aspects than in the drier and southerner aspects. Slope aspect in the study area was constructed using DEM and classified into nine categories including flat (1), North (0–22.5; 337.5–360), Northeast (22.5–67.5), East (67.5–112.5), Southeast (112.5–157.5), South (157.5–202.5), Southeast (202.5–247.5), West (247.5–292.5), and Northeast (292.5–337.5) (Fig. 3c).

3.2.4. Slope length

Slope length incorporated with slope-angle and affect the soil loss and hydrological processes of the mountain areas that can be considered an important factor in landslide activity (Pourghasemi and Rahmati, 2018). Slope length is the horizontal projection of the slope distance, which is measured along the slope surface (Wischmeier and Smith, 1978). In the current study, the slope-length (LS) factor can be calculated by the equation proposed by Moore and Burch (1986) as:

$$LS = 1.4 \left(\frac{A_s}{22.13} \right)^{0.6} \left(\frac{\sin \beta}{0.0896} \right)^{1.3} \quad (1)$$

Where, A_s is specific watersheds area (m^2/m) and β is slope angle (degree). In the current study, the LS factor was extracted from DEM using SAGA software (Fig. 3f).

3.2.5. Topographic wetness index (TWI)

The topographic wetness index represents a theoretical measure of the accumulation of flow at any point within a drainage basin and the tendency of the water to move downslope by gravitational forces. The topographic wetness index can be thought of as an abstract parameter to be used as a basis for estimating the local soil moisture status and thus land sliding areas due to surface topographic effects on hydrologic response. Soil moisture plays a vital role in slope instability, particularly for shallow landslides. According to Fredlund (1987), shallow landslides can occur on slopes when water from precipitation infiltrates the soil and eliminates the suction, and lowers the apparent cohesion. Modeling water in soil slopes in extensive areas is a difficult task as the soil water content is governed by several factors, some of which can only be estimated from laboratory tests (Kuriakose et al., 2009a). Since the topographic wetness index is intended to represent the topographic control on soil wetness, it is considered in this study as a proxy to soil water content. In the estimation of the wetness index, a depression-less DEM was calculated to remove the sinks in the image. After multiple flow directions were determined from the DEM, the flow accumulation area and tangent of the slope were calculated, spatially. The topographic wetness index (TWI) is defined as (Beven and Kirkby 1979; Moore et al., 1991):

$$TWI = \ln \left(\frac{A_s}{\tan \beta} \right) \quad (2)$$

Where A_s is the specific catchment area (SCA) and β is the local slope angle (in degrees). In the current study, the LS factor was extracted from DEM using SAGA software (Fig. 3g).

3.2.6. Stream Power Index (SPI)

The next type of DEM-derived topographic data used in this study is the Stream power index (SPI). This index is a measure of the erosive power of water flow based on the assumption that discharge (q) is proportional to a specific catchment area (A_s) (Eq. 2.2) (Moore et al., 1991).

$$SPI = A_s \tan \beta \quad (3)$$

Where A_s is the specific catchment's area (m^2/m), and b the slope angle (degree). SPI can be considered as one of the components of landslide occurrence (Lee and Min 2001; Yilmaz, 2009). In the current study, the LS factor was extracted from DEM using SAGA software (Fig. 3h).

3.2.7. Distance from drainage

Rivers composed of drainage network have negative impacts on landslide susceptibility since they abrade the slope base and saturate the underwater section of the material forming the slope (Pachauri et al., 1998; Dai et al., 2001; Cevik and Topal 2003; Ercanoglu and Gokceoglu 2003; Vijith and Madhu, 2008; Akgun and Turk 2010). The Euclidean distance tool in ArcGIS was used to produce distance from the faults map (Fig. 3m).

3.2.8. Plan Curvature

For shallow translational landslide, topography, particularly slope angle and convergence, plays an important role in controlling stability (Hennrich and Crozier, 2004). The plan curvature defines topographic convergence which is an important control on sub-surface flow concentration (Talebi et al., 2006). The influence of plan curvature on the slope erosion processes is the convergence or divergence of water during downhill flow and for this reason, this parameter constitutes one of the conditioning factors controlling landslide occurrence (Ercanoglu and Gokceoglu, 2003; Nefeslioglu et al. 2008; Oh and Pradhan, 2011). In this study, plan curvature was reclassified into three classes: convergent, parallel, and divergent. In the current work, plan and profile curvatures were extracted from the DEM using ArcGIS (Fig. 3d).

3.2.9. Profile Curvature

Field studies and numerical simulation have shown that bedrock profile curvature and hillslope plan shape are the most significant controls on sub-surface flow and saturation (Troch et al., 2003). Profile curvature refers to the rate of change of gradient and controls the acceleration and deceleration of near-surface flows. Talebi et al. (2008b) showed that the location of the critical slip surface is changed based on hillslope shape as it is located in the upstream part of the slope for the concave and in the downstream part of the slope for the convex profiles. Generally, Profile curvature affects the driving and resisting stresses within a landslide in the direction of motion and it controls the change of velocity of mass flowing down the slope. In this study, profile curvature reclassified into three classes: concave, flat, and convex. In the current work, plan and profile curvatures were extracted from the DEM using ArcGIS (Fig. 3e).

3.2.10. Geological Formation

Since different lithologic units have different landslide susceptibility values, this factor is very important in providing data for susceptibility mapping. For this reason, it is essential to group the lithologic properties properly (Carrara et al., 1991; Anbalagan 1992; Pachauri et al. 1998; Dai et al. 2001; Duman et al. 2006). In the study area, rock units exist from the cretaceous era to sediments of present amongst various lithological formations in the area, the marl, shale, and silt deposits are known to be the most susceptible to landslides (Table 2) (Fig. 3i).

3.2.11. Distance to faults

Investigations have shown that the probability of landslide occurrence is notably increased at those sites closer to lineaments (Greenbaum et al., 1995; Lee et al., 2002; Kanungo et al., 2006; Bucci et al., 2016). Lineaments not only affect surface material structures but can also make a large contribution to terrain permeability, favoring slope instability. Remote sensing techniques have proven to be very successful for the detection of geological lineaments (Suzen and Toprak, 1998). In this study, remote sensing techniques and the Euclidean distance tool in ArcGIS were used to produce distance from the faults map (Fig. 3n).

Table 2- Types of the geological formation of the study area.

Geological era	Code	Formation	Lithology
Quaternary	Qt	Alluvium	Alluvium and recent deposits
U. Pliocene	Lbm	Lahbari member	Alternation of light brown to grey marl and sandstone
Miocene	Gs	Gachsaran	Alternation of anhydrite and red to grey marl with interbedded limestone
Eocene-Oligocene	AS	Asmari	Cream, white well-bedded to massive limestone, dolomitic limestone, and marl
Paleocene-Eocene	Pd	Pabdeh	Alternation of gray, white shale, marly limestone, and marl
U.Cretaceous	Gu	Gurpi	Grey, blue shale, and marly limestone with pyrite
U.Cretaceous	Ehm	Emam hasan member	Grey, thick-bedded limestone with marl
U.Cretaceous	II-Sg	Ilam	Grey, white thin to medium bedded limestone with interbedded of shale
U.Cretaceous	Sg	Surgah	Grey, dark shale, and interbedded yellow marly limestone
U.Cretaceous	Sv	Sarvak	Grey, dark thin to massive bituminous limestone with dark shale

3.2.12. Land cover

Some researchers (Gokceoglu and Aksoy, 1996; van Beek et al., 2005; Devkota et al., 2013) emphasize the positive effects of dense vegetation on the stability of slopes. While other researchers (Greenway 1987; Wu and Sidle, 1995) also mention some negative effects of vegetation on slope stability. Theoretically tree roots reinforce the soil, increasing soil shear strength if the roots penetrate through the shear zone. In this study, land cover/land use map interpreted from an ASTER satellite image of DATE. Image classification was carried out using a pixel-based classification system with the artificial neural network (ANN) algorithm and cover/land use map classes include agriculture land, barren land, forest land, grassland, garden land, and water (Fig. 3j).

3.2.13. Normalized Difference Vegetation Index (NDVI)

A vegetation index is a measure of surface reflectance and gives a quantitative estimate of the vegetation growth and biomass (Hall et al., 1995) and shows the density of plant growth over the entire globe. The NDVI is an influencing variable in landslide susceptibility modeling (Althuwaynee et al., 2012). In general, the value of NDVI ranged from -1 to 1; the high the value the denser the vegetation cover. (Weier and Herring, 2005). Using the satellite image of ASTER, the NDVI was taken into the consideration as a landslide-related factor (Fig. 3k). The NDVI was calculated from the following formula:

$$NDVI = \left(\frac{IR - R}{IR + R} \right) \quad (4)$$

Where IR is the infrared portion of the electromagnetic spectrum, R is the red portion of the electromagnetic spectrum.

3.2.14. Distance to road

Similar to the effect of the distance to streams, landslides may occur on the road and the side of the slopes affected by roads (Sidle et al., 1985, Pachauri et al., 1998; Yalcin, 2005). This is mainly since the natural condition of the slope is damaged during the process of road construction. Also, the road cut exposes the joints and fractures that make the slope unstable. Road cuts are usually sites of anthropological instability (Pradhan, 2010b). The Euclidean distance tool in ArcGIS was used to produce distance from the faults map (Fig. 3).

4. Methods

The flowchart for landslide susceptibility mapping is shown in Fig. 4. In this study, the fourteen landslide conditioning factor maps were converted into a pixel format with a spatial resolution of 15×15 m. In each map, the frequency ratio value for each attribute class was calculated.

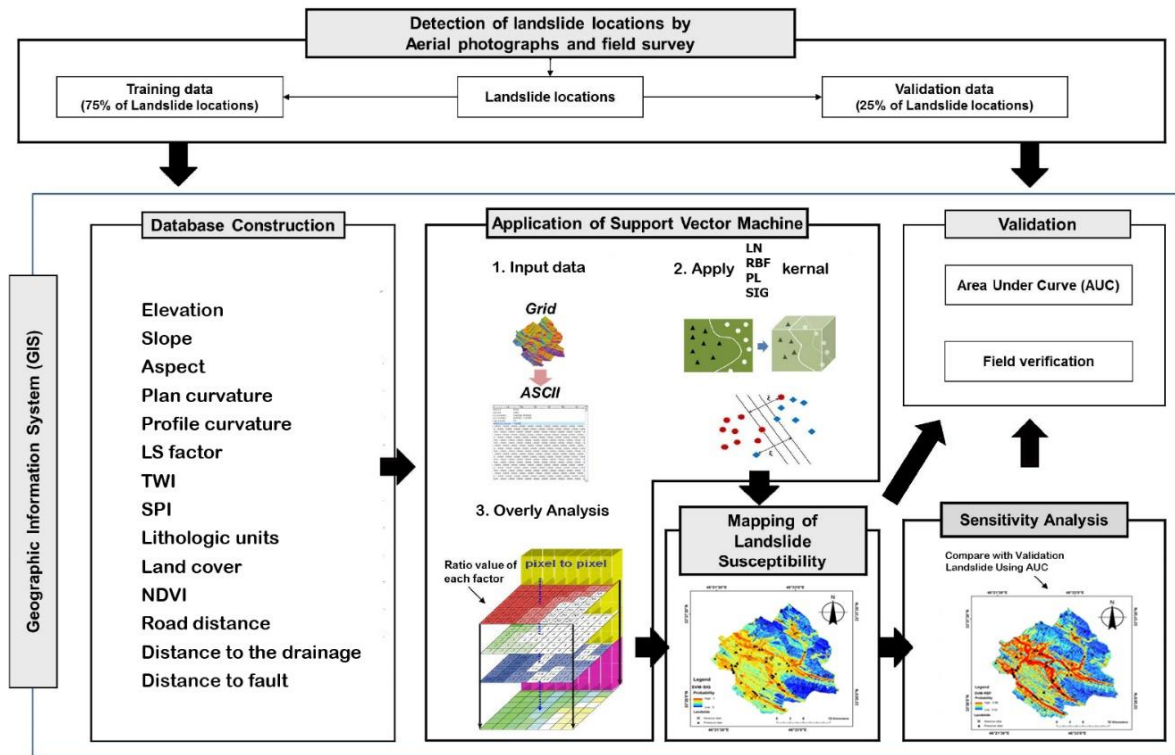


Fig. 4- Flowchart of the study

4.1. Preparation of the training and testing data set

In the first step, each attribute class was then assigned a sequence number based on the ratio value. In the next step, the Max-Min normalization procedure was carried out to rescale in the range 0.1 to 0.9 using Eq(5) (Wang and Huang, 2009):

$$x' = \frac{x - \text{Min}(x)}{\text{Max}(x) - \text{Min}(x)}(U - L) + L \tag{5}$$

Where x' is the normalized data matrix, x is the original data matrix, and U and L are the upper and lower normalization boundaries.

When developing the SVM, the data is commonly partitioned into at least two subsets such as training and test data. Before running the SVM program, the training site should be selected. On the other hand, it is expected that the training data include all the data belonging to the problem domain and, the test data should be different from those used in the training stage (Dixon, 2005). Although no exact mathematical rule to determine the required minimum size of these subsets exists, However, some suggestions for the portions of these samplings are encountered in the literature (Pradhan et al., 2011).

4.2. Support Vector Machines

Support vector machine is a supervised learning method based on statistical learning theory and the structural risk minimization principle (Vapnik, 2001). Using the training data, SVM implicitly maps the

original input space into a high dimensional feature space (Kanevski et al., 2009; Abe, 2010). Subsequently, in the feature space, the optimal hyperplane is determined by maximizing the margins of class boundaries (Abe, 2010). The training data that are closest to the optimal hyperplane are called support vectors. Once the decision surface is obtained, it can be used for classifying other data. Consider a training dataset of instance-label pairs (x_i, y_i) with $x_i \in R^n$, $y_i \in \{1, -1\}$ and $i=1, \dots, m$. In the current context of landslide susceptibility, x_i is a vector of input space that contains elevation, slope gradient, slope aspect, slope length, topographic wetness index, plan curvature, profile curvature, channel proximity, surface materials (substrate), distance to fault, land cover/land use, distance to road and NDVI. The two classes $\{1, -1\}$ denote landslide pixels and no-landslide pixels. The SVM classification aims to find an optimal separating hyperplane that can distinguish the two classes i.e., landslides and no-landslides $\{1, -1\}$ from the mentioned set of training data. For the case of linearly separable data, a separating hyperplane can be defined as:

$$y_i(w \times x_i + b) \geq 1 - \xi_i \tag{6}$$

Where w is a coefficient vector that determines the orientation of the hyperplane in the feature space, b is the offset of the hyperplane from the origin, ξ_i s the positive slack variables (Cortes and Vapnik, 1995).

The determination of an optimal hyperplane leads to the solving of the following optimization problem using Lagrangian multipliers:

$$\text{Minimize } \sum_{i=1}^n \alpha_i - \frac{1}{2} \sum_{i=1}^n \sum_{j=1}^n \alpha_i \alpha_j y_i y_j (x_i x_j) \tag{7}$$

$$\text{Subjects to } \sum_{i=1}^n \alpha_i y_i = 0 \text{ and } 0 \leq \alpha_i \leq C \tag{8}$$

Where α_i are Lagrange multipliers, C is the penalty, the slack variables (ξ_i) allow for penalized constraint violation. The decision function, which will be used for the classification of other data, can then be written as:

$$g(x) = \text{sign} \left(\sum_{i=1}^n y_i \alpha_i x_i + b \right) \tag{9}$$

In cases when it is impossible to find the separating hyperplane using the linear kernel function, the original input data may be transferred into a high dimensional feature space through some nonlinear kernel functions. The classification decision function is then written as:

$$g(x) = \text{sign} \left(\sum_{i=1}^n y_i \alpha_i K(x_i, x_j) + b \right) \tag{10}$$

Where $K(x_i, x_j)$ is the kernel function. The choice of the kernel function is crucial for successful SVM training and classification accuracy (Damasevicius, 2010; Pradhan, 2013). There are four types of kernel function groups that are commonly used in SVM: LN, PL, RBF, and SIG (Yao et al., 2008b). Table 3 shows SVM Kernel functions and their parameters used in this study. γ is the gamma term in the kernel function for all kernel types except LN, d is the polynomial degree term in the kernel function for the PL and r is the bias term in the kernel function for the PL and SIG (Pradhan, 2013). In the present study, the non-linear two-class SVM method was used, because Yao et al., (2008) had reported that a more accurate susceptibility map was produced from the two-class.

Table 3- Kernel functions and their parameters are used in this study.

Kernel	Formula	Kernel parameters
Linear kernel function (LN)	$K(x_i, x_j) = x_i^T x_j$	-
Radial basis function (RBF)	$K(x_i, x_j) = \exp(-\gamma \ x_i - x_j\ ^2)$	γ, d
Polynomial function (PL)	$K(x_i, x_j) = (-\gamma x_i^T x_j + D)^d$	γ
Sigmoid kernel function (SIG)	$K(x_i, x_j) = \text{Tanh}(-\gamma x_i^T x_j + D)^d$	γ

4.3. Model Performance Evaluation

Using several statistical evaluation criteria such as true positive (TP), false positive (FP), true negative (TN), false negative (FN). The overall accuracy of the trained landside susceptibility model is calculated as $(TP+TN)/N$, with N as the total number of training pixels. The reliability of the landside susceptibility model is estimated using Cohen's Kappa index (κ) (Guzzetti et al., 2006) as follows:

$$K = \frac{P_{obs} - P_{exp}}{1 - P_{exp}} \quad (11)$$

Where $P_{obs} = (TP+TN)/N$ is the proportion of pixels that are correctly classified as landslide or non-landslide. $P_{exp} = ((TP+FN)(TP+FP) + (FP+TN)(FN+TN))/N^2$ is the proportion of pixels for which the agreement is expected by chance. According to Values proposed by Landis and Koch (1977), the strength of agreement between the model and the reality is as follows: ≤ 0 (poor); 0-0.2 (slight); 0.2-0.4 (fair); 0.4-0.6 (moderate); 0.6-0.8 (substantial); 0.8-1 (almost perfect).

The classification capabilities of the SVM and other classifiers have been tested through the use of receiver operating characteristic (ROC) graphs and prediction rate curves. The ROC (Egan, 1975; Fawcett, 2006) is a graphical analysis of the success rate of binary classification and it provides useful information about the proneness of a model to generate false positives errors. The result of the ROC analysis is summarized by the area under the curve (AUC), which expresses a complete success in classification for an AUC = 1, and random classification for an AUC = 0.5.

The prediction rate curves method (Chung and Fabbri, 1999; van Westen et al., 2008), has been widely applied for many years to assess the quality of susceptibility mapping.

5. Results

5.1. Application of support vector machines model

The landslide inventory map with 45 landslide polygons was randomly split into two parts: Part1 with 75% of the data (34 landslides) used in the training phase of the landslide models. Part-2 is a validation dataset with 25% of the data (11 landslides). A total of landslide pixels in part1 were assigned the value of 1, and the same amount of no-landslide pixels was randomly generated from the landslide-free area and assigned the value -1. Fourteen landslide conditioning factors were considered that include: elevation, slope gradient, slope aspect, slope length, topographic wetness index (TWI), Stream Power Index (SPI), plan curvature, profile curvature, distance from drainage, surface materials, distance to fault, land cover, distance to road and NDVI. The results of the spatial relationship between landslides and conditioning factors using the frequency ratio model are shown in Table 4.

The performance of the SVM model is depended on the selection of kernel functions and their parameters. In this research, a support vector machine with 4 types of kernels classifiers such as linear kernel (LN), polynomial kernel (PL), radial basis function (RBF) kernel, and sigmoid kernel (SIG) were used in GIS for landslide susceptibility mapping. Cohen's Kappa indexes are 0.93, 0.91, 0.84, and 0.82 for the four landslide models (Table 5). The Kappa values indicate that the strength agreement between

the observed and the predicted values are substantial for SVM-LN and SVM-SIG. Whereas it is almost perfect for SVM-RBF, SVM-PL. Once the landslide susceptibility models were successfully trained, they were then used to calculate the landslide susceptibility indexes (LSI). In the present study, the non-linear two-class SVM method was used, the two-class SVM requires both absence and presence data to train the model. Four susceptibility mapping results using SVM modeling with various kernel functions in GIS are shown in Fig. 5. The landslide susceptibility probability value (LSPV) ranges from 0 to 1, with 0 indicating no probability of a landslide and 1 certainty of a landslide.

Table 4- Normalized classes of landslide conditioning factors used.

Domain	Class	Class pixels (%)	Landslide pixels (%)	Frequency ratio	Normalized classes
Elevation(m)	900-1400	40.38	73.39	1.82	0.90
	1400-1900	47.47	25.80	0.54	0.34
	1900-2400	11.29	0.80	0.07	0.13
	>2400	0.86	0.00	0.00	0.10
Slope Angle(degree)	0-15	37.75	35.32	0.94	0.17
	15-30	29.80	25.04	0.84	0.10
	30-45	18.52	17.43	0.94	0.18
	45-65	10.38	15.43	1.49	0.58
	>65	3.55	6.77	1.91	0.90
Slope Aspect	Flat	0.00	0.00	0.00	0.10
	N	12.23	16.38	1.34	0.61
	NE	13.93	29.59	2.12	0.90
	E	8.04	14.26	1.77	0.77
	SE	8.04	6.44	0.80	0.40
	S	14.08	6.64	0.47	0.28
	SW	22.41	4.61	0.21	0.18
	W	12.50	9.24	0.74	0.38
Slope length	NW	8.77	12.85	1.46	0.65
	0-4	36.91	33.32	0.90	0.13
	4-8	23.91	21.78	0.91	0.14
	8-12	16.51	14.47	0.88	0.10
	12-16	14.59	17.36	1.19	0.43
	16-20	6.66	10.88	1.64	0.90
TWI	>20	1.42	2.19	1.54	0.80
	<4	73.07	79.53	1.09	0.90
	10-15	24.42	19.24	0.79	0.52
	15-20	2.21	1.09	0.49	0.14
SPI	>20	0.31	0.14	0.46	0.10
	0-25	37.08	33.67	0.91	0.10
	25-50	18.08	18.39	1.02	0.46
	50-75	11.24	12.70	1.13	0.84
	75-100	7.11	8.17	1.15	0.90
Plan curvature	>100	26.48	27.07	1.02	0.48
	Divergent	11.75	10.18	0.87	0.09
	Parallel	70.86	69.80	0.98	0.43
Profile curvature	Convergent	17.39	20.03	1.15	0.90
	Convex	6.58	11.29	1.72	0.90
	Straight	79.42	75.93	0.96	0.15
	Concave	14.00	12.78	0.91	0.10

Distance to drainages (m)	0-100	4.95	21.46	4.33	0.81	
	100-200	6.49	31.57	4.86	0.90	
	200-300	15.46	17.51	1.13	0.27	
	300-400	29.81	23.79	0.80	0.21	
	>400	43.28	5.68	0.13	0.10	
Distance to fault(m)	0-1000	18.34	13.74	1.33	0.74	
	1000-2000	22.30	15.50	1.44	0.84	
	2000-3000	25.60	16.96	1.51	0.90	
	>3000	33.75	53.81	0.63	0.10	
Rock formation	Alluvium	9.99	10.41	0.96	0.38	
	Asmari	1.08	9.38	0.12	0.13	
	Emam hasan member	0.20	4.25	0.05	0.11	
	Gachsaran	0.02	0.87	0.02	0.11	
	Gurpi	33.70	17.18	1.96	0.67	
	Ilam	23.43	12.94	1.81	0.62	
	Lahbari member (old					
	landslides)	19.05	6.89	2.76	0.90	
	Pabdeh	10.28	26.25	0.39	0.21	
	Sarvak	0.00	10.00	0.00	0.10	
	Surgah	2.26	1.84	1.23	0.46	
	Landcover/Landuse	Lake	0.65	0.16	0.25	0.11
		Horticulture	0.75	0.17	0.23	0.10
		Dry farming	2.74	4.43	2.00	0.71
Rangeland		54.21	54.01	0.98	0.44	
Forest		27.92	13.20	0.47	0.21	
Barren land		13.74	28.03	2.04	0.90	
NDVI	-0.27-0.1	9.93	12.76	1.28	0.90	
	-0.1-0	71.09	86.61	1.22	0.86	
	0-0.1	17.23	0.59	0.03	0.11	
	0.1-0.2	1.26	0.03	0.02	0.10	
	>0.2	0.49	0.01	0.02	0.10	
Distance to roads(m)	0-100	5.51	19.16	3.48	0.90	
	100-200	5.12	15.02	2.93	0.75	
	200-300	4.92	10.71	2.18	0.53	
	300-400	4.52	4.24	0.94	0.18	
	>400	79.93	50.86	0.64	0.10	

Table 5- Cohen’s Kappa index for the four SVM models.

Parameter	SVM-RBF	SVM-PL	SVM-LN	SVM-SIG
Cohen’s Kappa index	0.93	0.91	0.84	0.82

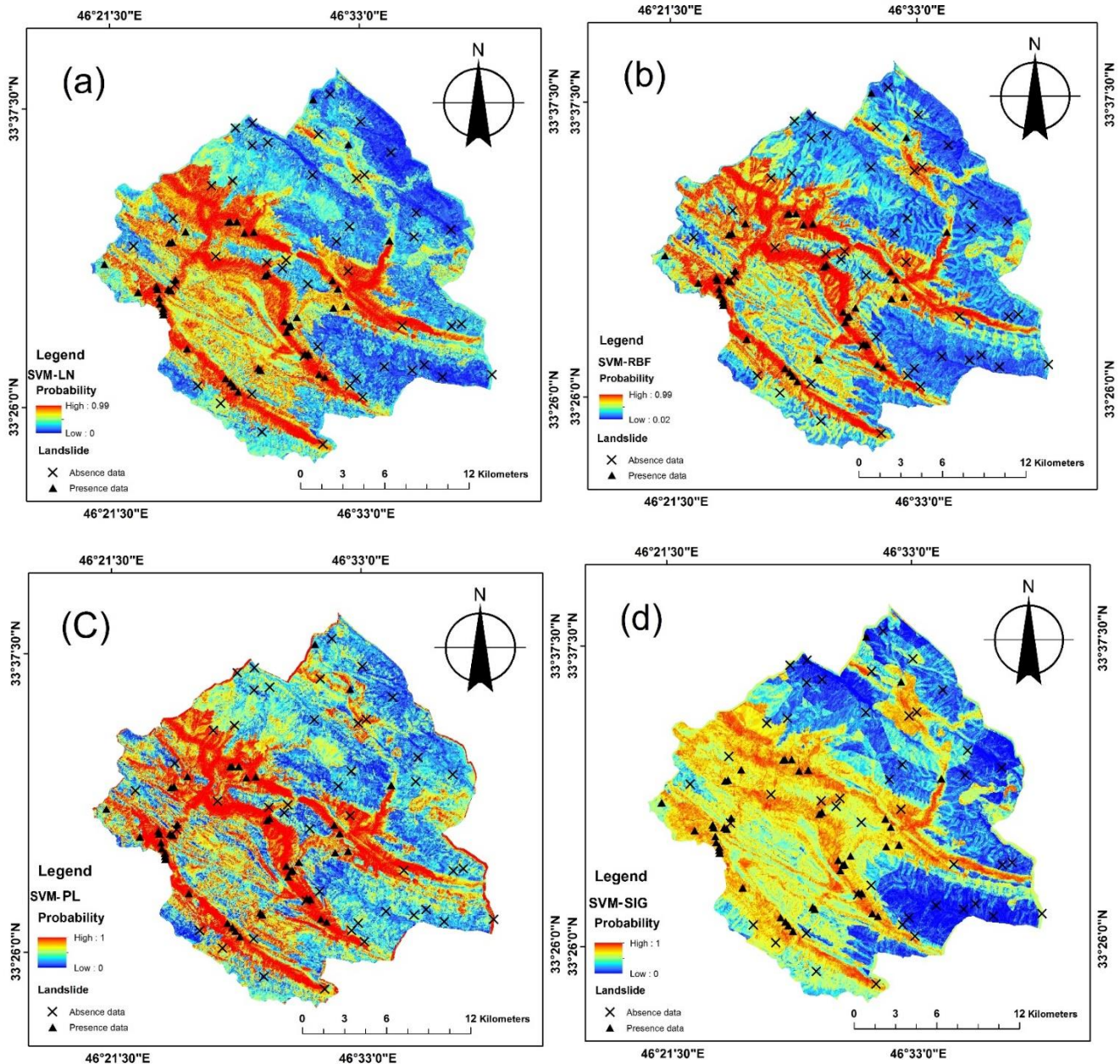
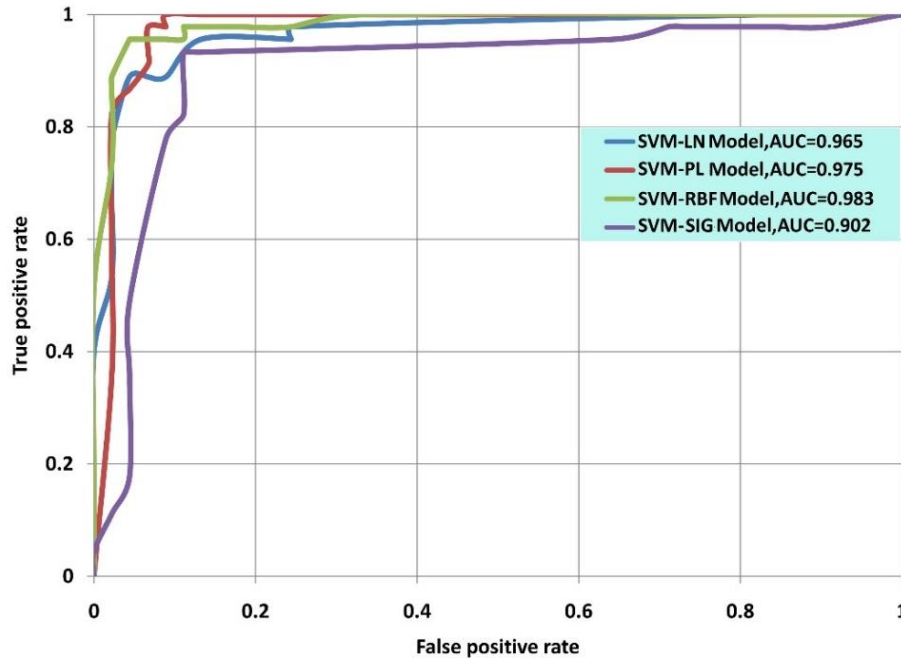


Fig. 5- Susceptibility map as predicted by the SVM model. (a) SVM-LN; (b) SVM-RBF; (c) SVM-PL; (d) SVM-SIG.

5.2. Validation and comparison of landslide susceptibility maps

The four landslide susceptibility maps were validated using the success-rate and prediction-rate curves (Chung et al., 2003; Guzzetti et al., 2006). The success rate results were obtained by comparing the four landslide susceptibility maps with the landslide pixels in the training dataset (Fig 6). The result shows that SVM-RBF and SVM-PL have the highest area under the curve (AUC) values of 0.983 and 0.975 respectively. They are followed by SVM-LN (0.965) and SVM-SIG (0.902). The AUC results indicate that the capacity of correctly classifying the areas with existing landslides is highest for SVM-RBF, followed by the SVM-PL, SVM-LN, SVM-SIG. In this study, the prediction-rate curves and area under

the curves were obtained (Fig 7) by comparing the four susceptibility maps with the landslide pixels in the validation dataset. The results show that the highest prediction capability is for SVM-RBF and SVM-PL with AUC values of 0.946 and 0.931 respectively, followed by SVM-LN (0.912) and SVM-SIG (0.871).



(0.871). Compared with the results from the SVM-LN and SVM-SIG models, the prediction capability of the two SVM-RBF and SVM-PL models seems to be slightly better.

Fig. 6- Success rate curves of the four SVM models

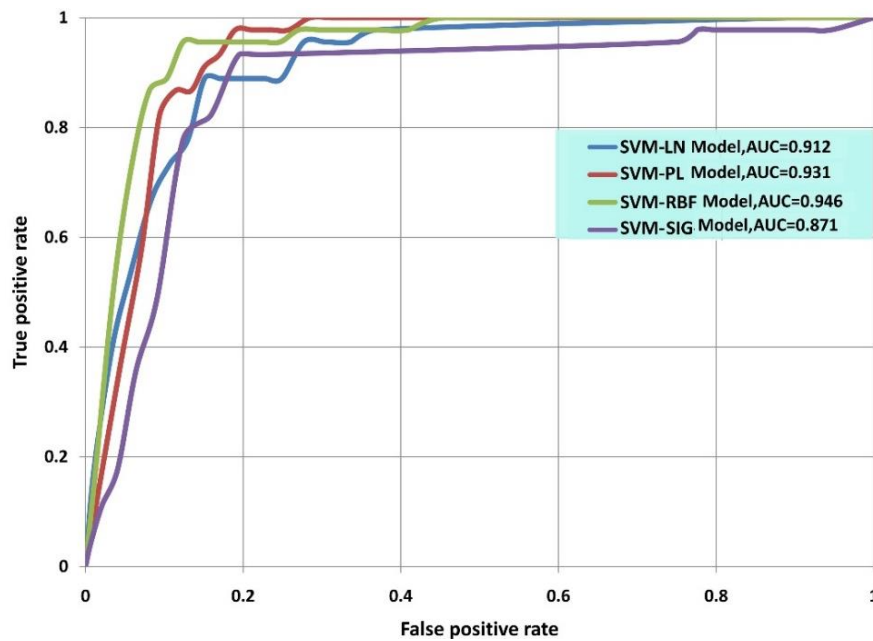


Fig. 7- Prediction rate curves of the four SVM models

5.3. Reclassification of landslide susceptibility indexes and relative importance assessment of landslide conditioning factors

For visual interpretation of landslide susceptibility probability value maps, the necessity of classifying data into categorical susceptibility classes arose. In this study, the quintile data classification approach was chosen, and the landslide susceptibility index map was classified into five susceptibility classes: very low, low, moderate, high, and very high. Landslide density analysis was performed on the five landslide susceptibility classes. The results show that the landslide density gradually increases from the very low to the very high susceptibility class in SVM- RBF, SVM-PL, and SVM- LN (Fig 8).

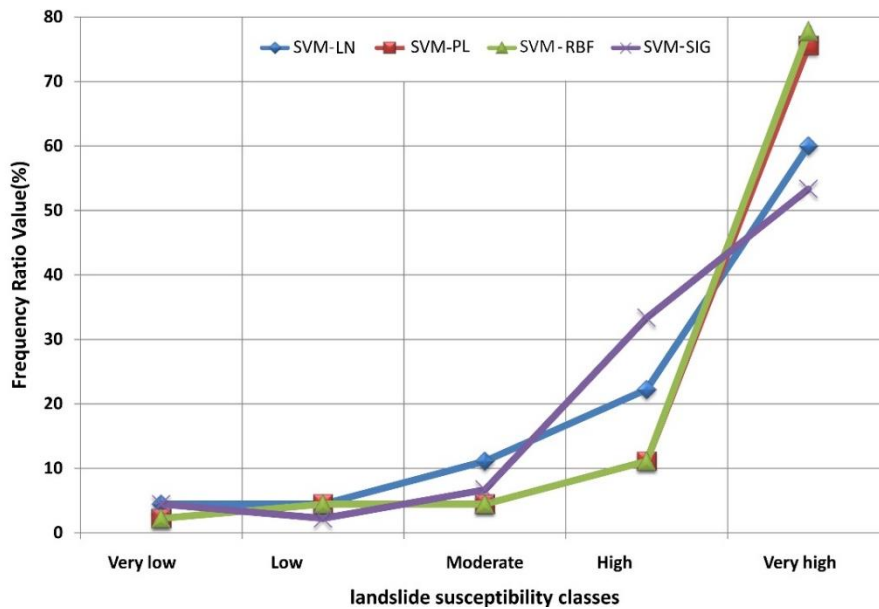


Fig. 8- Frequency ratio plots of four landslide susceptibility classes of the SVM models.

In the next stage, a separate comparison was made between the three susceptibility maps according to the landslide susceptibility zones. Frequency ratio analysis was carried out on the classification results and landslide location data of the corresponding histograms (Fig 9).

The importance of a certain factor was estimated by excluding the factor and then calculated the Cohen’s kappa index of the model (Table 6). It could be observed that the highest accuracy was obtained when all of the fourteen factors are used, with SVM- LN, SVM-RBF, SVM-PL. However, the distance to roads, distance to drainages, plan curvature, topographic wetness index (TWI), and slope length are the most important factors for SVM- LN. In the case of SVM-RBF, the most important factor is the distance to roads. Whereas distance to roads, distance to rivers, plan curvature, and topographic wetness index (TWI) is most important for SVM-PL. And the distance to roads, distance to drainages, plan curvature and slope angle are most important for SVM- SIG.

Table 6. Accuracy of the trained SVM models for landslide susceptibility using all conditioning factors and without one of the factors.

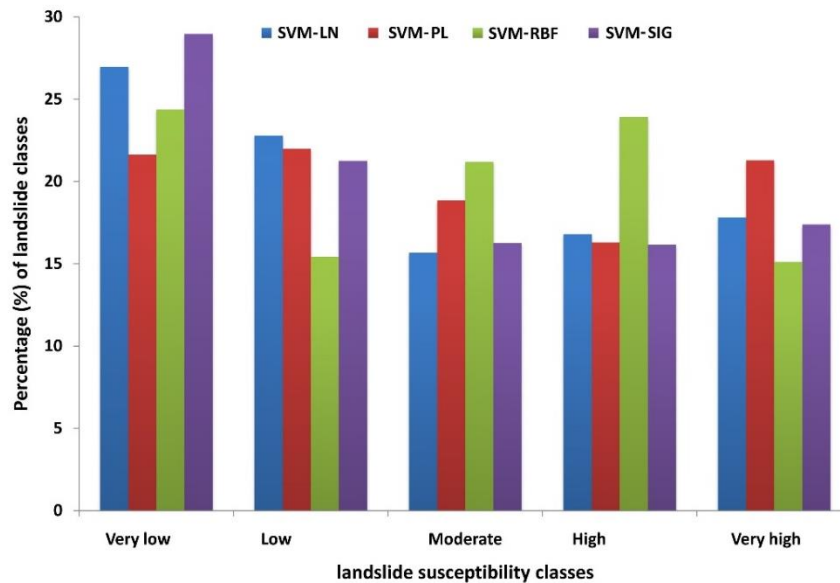


Fig. 9- Frequency ratio plots of five landslide susceptibility classes of the SVM models.

Table 6- Accuracy of the trained SVM models for landslide susceptibility using all conditioning factors and without one of the factors.

No	Conditioning factor	Cohen's Kappa index			
		SVM- LN	SVM - RBF	SVM - PL	SVM - SIG
1	Without Elevation	0.86	0.91	0.91	0.82
2	Without Slope Angle	0.86	0.93	0.91	0.80
3	Without Slope Aspect	0.86	0.93	0.91	0.84
4	Without Slope Length	0.84	0.91	0.93	0.84
5	Without TWI	0.84	0.93	0.88	0.82
6	Without SPI	0.86	0.93	0.91	0.82
7	Without Plan curvature	0.84	0.93	0.88	0.80
8	Without Profile curvature	0.86	0.93	0.93	0.84
9	Without Distance to drainages	0.83	0.91	0.88	0.77
10	Without Distance to fault	0.86	0.91	0.91	0.82
11	Without Geology formation	0.86	0.91	0.91	0.84
12	Without Land cover	0.86	0.91	0.91	0.82
13	Without NDVI	0.86	0.93	0.93	0.84
14	Without Distance to roads	0.82	0.89	0.85	0.73

6. Discussion and Conclusions

Landslide susceptibility can be assessed from different methods based on GIS technology. Especially in the last years, many research papers were published to solve deficiencies and difficulties in the assessment of susceptibility. It should be aimed that the procedure for preparing landslide susceptibility maps must be as simple and accurate as possible. In this study, we investigated the potential application

of two-class SVM to predict the potential distribution of landslides in natural terrain located on the Ilam dam watershed of Iran. Fourteen landslide conditioning factors (slope gradient, slope aspect, slope length, topographic wetness index (TWI), Stream Power Index (SPI), plan curvature, profile curvature, distance from drainage, surface material, distance to fault, land cover/land use, distance to road and NDVI were employed) were used in this analysis. The landslide inventory with 45 landslide-polygons that occurred during the last ten years was used. 75% of the landslide inventory was used for building susceptibility models, whereas the remaining 25% was used for validating and assessing the prediction capability of the models. Four kernel functions were included in the analysis, LN RBF, PL, and SIG. Four landslide susceptibility maps were constructed. The landslide susceptibility maps were validated and compared using the success-rate and the prediction-rate methods. The largest area under the success-rate curve (AUC) is for the SVM-RBF (0.983), followed by SVM-PL (0.957), SVM-LN (0.965), and SVM-SIG (0.902). It indicates that SVM-RBF and SVM-PL have better goodness of fit to the training data. The highest area under the prediction-rate curve (AUC) is for SVM-RBF (0.946) and SVM-PL (0.931), followed by SVM-LN (0.912), SVM-SIG (0.871). The reliability of the four susceptibility models was assessed using Cohen's Kappa index (κ). κ values are 0.93, 0.91 for SVM-RBF, SVM-PL respectively, indicating almost perfect agreement. Whereas κ values for SVM-LN, SVM-SIG is 0.87, and 0.84 indicating that the strength of agreement between the observed and predicted values are substantial. The findings of this study agree with Pourghasemi et al., 2013c who states that SVM-RBF and SVM-PL possess slightly better prediction efficiency than other kernel function.

Moreover, the influences of factors on the landslide susceptibility map were evaluated by using Cohen's kappa index of the model. Although all factors used in this study have positive influences on landslide susceptibility analysis the result showed that the distance to roads, distance to drainages and plan curvature are the most important causative factors in landslide occurrence. Similarly, the results also agree with Zhao and Zhao, 2021; who concluded distance to roads, rivers, and topography have positive effect on landslide occurrence.

In a conclusion, the results show that SVM together with GIS is a powerful tool for landslide susceptibility mapping. These maps can be very useful for natural hazards assessment and land use planning. The findings of this study are comparable to those obtained in other studies, such as Brenning, 2005; Yao et al, 2008; Yilmaz, 2010; Marjanovic et al, 2011; Ballabio and Sterlacchini, 2012; Pourghasemi et al., 2013c. In summary, SVM has a significant advantage when compared to other algorithms: the uniqueness of the solution (Pourghasemi et al., 2020). However, the SVM does not offer many choices for controlling values, neither does it directly provide probability and statistics estimates in the results and procedure, as it is a non-parametric technique.

Additionally, as the reservoir of the dam in this study is located in the landslide susceptibility, risk, and management zone of very high, the damages caused by the occurrence of this phenomenon in this region (reservoir) including filling of the reservoir by sediments transported by landslides, damages to the body and weir of dam and condition of the downstream watershed have to be studied and estimated in detail. Finally, we recommend using other landslide susceptibility zoning models with other predisposing factors such as soil depth and type, soil moisture along the present research parameters (through different classification such as physically-based models). Applying risk assessment algorithms and landslide management, as well as the present numerical models, are also advised.

Acknowledgments

The authors are grateful to the anonymous reviewers for their valuable comments to improve the manuscript.

Declarations

Funding Information: (Private funding by authors)

Conflict of Interest /Competing interests: (None)

REFERENCES

- Abe, S. (2005). Support vector machines for pattern classification (Vol. 2, p. 44). London: Springer.
- Adition, A., Kubota, T., & Shinohara, Y. (2018). Comparison of GIS-based landslide susceptibility models using frequency ratio, logistic regression, and artificial neural network in a tertiary region of Ambon, Indonesia. *Geomorphology*, 318, 101-111. <https://doi.org/10.1016/j.geomorph.2018.06.006>
- Akgun, A., & Türk, N. (2010). Landslide susceptibility mapping for Avvalik (Western Turkey) and its vicinity by multicriteria decision analysis. *Environmental Earth Sciences*, 61(3), 595-611. <https://doi.org/10.1007/s12665-009-03731>
- Althuwaynee, O. F., Pradhan, B., & Lee, S. (2012). Application of an evidential belief function model in landslide susceptibility mapping. *Computers & Geosciences*, 44, 120-135. <https://doi.org/10.1016/j.cageo.2012.03.003>
- Anbalagan, R. (1992). Landslide hazard evaluation and zonation mapping in mountainous terrain. *Engineering geology*, 32(4), 269-277. [https://doi.org/10.1016/0013-7952\(92\)90053-2](https://doi.org/10.1016/0013-7952(92)90053-2)
- Ballabio, C., & Sterlacchini, S. (2012). Support vector machines for landslide susceptibility mapping: the Staffora River Basin case study, Italy. *Mathematical geosciences*, 44(1), 47-70. <https://doi.org/10.1007/s11004-011-9379-9>
- Bednarik, M., Yilmaz, I., & Marschalko, M. (2012). Landslide hazard and risk assessment: a case study from the Hlohovec–Sered’landslide area in south-west Slovakia. *Natural hazards*, 64(1), 547-575. <https://doi.org/10.1007/s11069-012-02577>
- Beven, K. J., & Kirkby, M. J. (1979). A physically based, variable contributing area model of basin hydrology/Un modèle à base physique de zone d'appel variable de l'hydrologie du bassin versant. *Hydrological Sciences Journal*, 24(1), 43-69. <https://doi.org/10.1080/02626667909491834>
- Bonham-Carter, G.F. (2002). Geographic information systems for geoscientists: Modelling with GIS. In: Merriam, D.F. (Ed.). *Computer Methods in the Geosciences*, vol. 13. Pergamon/Elsevier, New York, pp. 302–334.
- Brenning, A. (2005). Spatial prediction models for landslide hazards: review, comparison and evaluation. *Natural Hazards and Earth System Sciences*, 5(6), 853-862. <https://doi.org/10.5194/nhess-5-853-2005>
- Bucci, F., Santangelo, M., Cardinali, M., Fiorucci, F., & Guzzetti, F. (2016). Landslide distribution and size in response to Quaternary fault activity: the Peloritani Range, NE Sicily, Italy. *Earth Surface Processes and Landforms*, 41(5), 711-720. <https://doi.org/10.1002/esp.3898>
- Budimir, M. E. A., Atkinson, P. M., & Lewis, H. G. (2015). A systematic review of landslide probability mapping using logistic regression. *Landslides*, 12(3), 419-436. <https://doi.org/10.1007/s10346-014-0550-5>
- Bui, D. T., Pradhan, B., Lofman, O., & Revhaug, I. (2012a). Landslide susceptibility assessment in vietnam using support vector machines, decision tree, and Naive Bayes Models. *Mathematical problems in Engineering*, 2012. <https://doi.org/10.1155/2012/974638>
- Bui, D. T., Pradhan, B., Lofman, O., Revhaug, I., & Dick, O. B. (2012b). Landslide susceptibility mapping at Hoa Binh province (Vietnam) using an adaptive neuro-fuzzy inference system and GIS. *Computers & Geosciences*, 45, 199-211. <https://doi.org/10.1016/j.cageo.2011.10.031>
- Bui, D. T., Tuan, T. A., Klempe, H., Pradhan, B., & Revhaug, I. (2016). Spatial prediction models for shallow landslide hazards: a comparative assessment of the efficacy of support vector machines, artificial neural networks, kernel logistic regression, and logistic model tree. *Landslides*, 13(2), 361-378. <https://doi.org/10.1007/s10346-015-0557-6>
- Bui, D. T., Tuan, T. A., Hoang, N. D., Thanh, N. O., Nguyen, D. B., Van Liem, N., & Pradhan, B. (2017). Spatial prediction of rainfall-induced landslides for the Lao Cai area (Vietnam) using a hybrid intelligent approach of least squares support vector machines inference model and artificial bee colony optimization. *Landslides*, 14(2), 447-458. <https://doi.org/10.1007/s10346-016-0711-9>
- Burrough, P. A. (1986). Principles of geographical. *Information systems for land resource assessment*. Clarendon Press, Oxford. <https://doi.org/10.1080/10106048609354060>
- Carrara, A., Cardinali, M., Detti, R., Guzzetti, F., Pasqui, V., & Reichenbach, P. (1991). GIS techniques and statistical models in evaluating landslide hazard. *Earth surface processes and landforms*, 16(5), 427-445. <https://doi.org/10.1002/esp.3290160505>
- Cevik, E., & Topal, T. (2003). GIS-based landslide susceptibility mapping for a problematic segment of the natural gas pipeline, Hendek (Turkey). *Environmental geology*, 44(8), 949-962. <https://doi.org/10.1007/s00254-003-0838-6>

- Chen, W., Pourghasemi, H. R., Panahi, M., Kornejady, A., Wang, J., Xie, X., & Cao, S. (2017). Spatial prediction of landslide susceptibility using an adaptive neuro-fuzzy inference system combined with frequency ratio, generalized additive model, and support vector machine techniques. *Geomorphology*, 297, 69-85. <https://doi.org/10.1016/j.geomorph.2017.09.007>
- Chung, C. J. F., Fabbri, A. G., & Van Westen, C. J. (1995). Multivariate regression analysis for landslide hazard zonation. In *Geographical information systems in assessing natural hazards* (pp. 107-133). Springer, Dordrecht. https://doi.org/10.1007/978-94-015-8404-3_7
- Chung, C. J. F., & Fabbri, A. G. (1999). Probabilistic prediction models for landslide hazard mapping. *Photogrammetric engineering and remote sensing*, 65(12), 1389-1399.
- Clerici, A., Perego, S., Tellini, C., & Vescovi, P. (2002). A procedure for landslide susceptibility zonation by the conditional analysis method. *Geomorphology*, 48(4), 349-364. [https://doi.org/10.1016/S0169-555X\(02\)00079-X](https://doi.org/10.1016/S0169-555X(02)00079-X)
- Colkesen, I., Sahin, E. K., & Kavzoglu, T. (2016). Susceptibility mapping of shallow landslides using kernel-based Gaussian process, support vector machines and logistic regression. *Journal of African Earth Sciences*, 118, 53-64. <https://doi.org/10.1016/j.jafrearsci.2016.02.019>
- Cooke, R. V., & Doornkamp, J. C. (1990). *Geomorphology in environmental management: a new introduction*. Oxford University Press (OUP).
- Cortes, C., & Vapnik, V. (1995). Support-vector networks. *Machine learning*, 20(3), 273-297. <https://doi.org/10.1007/BF00994018>
- Dahal, R. K., Hasegawa, S., Nonomura, A., Yamanaka, M., Masuda, T., & Nishino, K. (2008). GIS-based weights-of-evidence modelling of rainfall-induced landslides in small catchments for landslide susceptibility mapping. *Environmental Geology*, 54(2), 311-324. <https://doi.org/10.1007/s00254-007-0818-3>
- Dai, F. C., Lee, C. F., Li, J. X. Z. W., & Xu, Z. W. (2001). Assessment of landslide susceptibility on the natural terrain of Lantau Island, Hong Kong. *Environmental Geology*, 40(3), 381-391. <https://doi.org/10.1007/s002540000163>
- Damaševičius, R. (2010). Optimization of SVM parameters for recognition of regulatory DNA sequences. *Top*, 18(2), 339-353. <https://doi.org/10.1007/s11750-010-0152-x>
- DeGraff, J. V. (1979). Initiation of shallow mass movement by vegetative-type conversion. *Geology*, 7(9), 426-429. [https://doi.org/10.1130/0091-7613\(1979\)7<426:IOSMMB>2.0.CO;2](https://doi.org/10.1130/0091-7613(1979)7<426:IOSMMB>2.0.CO;2)
- Devkota, K. C., Regmi, A. D., Pourghasemi, H. R., Yoshida, K., Pradhan, B., Rvu, I. C., & Althuwaynee, O. F. (2013). Landslide susceptibility mapping using certainty factor, index of entropy and logistic regression models in GIS and their comparison at Mugling–Naravanghat road section in Nepal Himalaya. *Natural hazards*, 65(1), 135-165. <https://doi.org/10.1007/s11069-012-0347-6>
- Duman, T. Y., Can, T., Gokceoglu, C., Nefeslioglu, H. A., & Sonmez, H. (2006). Application of logistic regression for landslide susceptibility zoning of Cekmece Area, Istanbul, Turkey. *Environmental Geology*, 51(2), 241-256. <https://doi.org/10.1007/s00254-006-0322-1>
- Ercanoğlu, M., & Gokceoglu, C. (2003). Landslide Susceptibility Zoning of North Yenice (NW Turkey) by Multivariate Statistical Techniques. *Natural Hazard* 00(00):1-23. <https://doi.org/10.1023/B:NHAZ.0000026786.85589.4a>
- Ermini, L., Catani, F., & Casagli, N. (2005). Artificial neural networks applied to landslide susceptibility assessment. *Geomorphology*, 66(1-4), 327-343. <https://doi.org/10.1016/j.geomorph.2004.09.025>
- Fawcett, T. (2006). An introduction to ROC analysis. *Pattern recognition letters*, 27(8), 861-874. <https://doi.org/10.1016/j.patrec.2005.10.010>
- Fredlund, D.G. (1987). Slope stability analysis incorporating the effect of soil suction, in Anderson MG, and Richards KS, eds., Slope stability: geotechnical engineering and geomorphology: Chichester, UK. John Wiley & Sons, p. 113-144.
- Gheshlaghi, H. A., & Feizizadeh, B. (2017). An integrated approach of analytical network process and fuzzy based spatial decision making systems applied to landslide risk mapping. *Journal of African Earth Sciences*, 133, 15-24. <https://doi.org/10.1007/978-1-84996-098-4>
- Ghorbanzadeh, O., Blaschke, T., Gholamnia, K., Meena, S. R., Tiede, D., & Arval, J. (2019). Evaluation of different machine learning methods and deep-learning convolutional neural networks for landslide detection. *Remote Sensing*, 11(2), 196. <https://doi.org/10.3390/rs11020196>
- Gokceoglu, C., & Aksoy, H. Ü. S. E. Y. İ. N. (1996). Landslide susceptibility mapping of the slopes in the residual soils of the Mengen region (Turkey) by deterministic stability analyses and image processing techniques. *Engineering Geology*, 44(1-4), 147-161. [https://doi.org/10.1016/S0013-7952\(97\)81260-4](https://doi.org/10.1016/S0013-7952(97)81260-4)
- Goetz, J. N., Guthrie, R. H., & Brenning, A. (2011). Integrating physical and empirical landslide susceptibility models using generalized additive models. *Geomorphology*, 129(3-4), 376-386. <https://doi.org/10.1016/j.geomorph.2011.03.001>
- Gordo, C., Zêzere, J. L., & Marques, R. (2019). Landslide susceptibility assessment at the basin scale for rainfall-and earthquake-triggered shallow slides. *Geosciences*, 9(6), 268. <https://doi.org/10.3390/geosciences9060268>

- Graff, J., & Romesburg, H. (1980). Regional landslide-susceptibility assessment for wildland management: a matrix approach. In: Coates, D., Vitek, J. (Eds.). *Thresholds in Geomorphology*. George Allen and Unwin, London, pp. 401–414. <https://doi.org/10.4324/9781003028697-19>
- Greenbaum, D., Tutton, M., Bowker, M. R., Browne, T. J., Buleka, J., Grealley, K. B., & Tragheim, D. G. (1995). Rapid methods of landslide hazard mapping: Papua New Guinea case study.
- Greenway, D.R. (1987). Vegetation and slope stability. In: Anderson MG, Richards KS (eds) *Slope stability*. Wiley, New York, pp 187–230.
- Gritzner, M. L., Marcus, W. A., Aspinall, R., & Custer, S. G. (2001). Assessing landslide potential using GIS, soil wetness modeling and topographic attributes, Payette River, Idaho. *Geomorphology*, 37(1-2), 149–165. [https://doi.org/10.1016/S0169-555X\(00\)00068-4](https://doi.org/10.1016/S0169-555X(00)00068-4)
- Günther, A., Van Den Eeckhaut, M., Malet, J. P., Reichenbach, P., & Hervás, J. (2014). Climate-physiographically differentiated Pan-European landslide susceptibility assessment using spatial multi-criteria evaluation and transnational landslide information. *Geomorphology*, 224, 69–85. <https://doi.org/10.1016/j.geomorph.2014.07.011>
- Guzzetti, F., Carrara, A., Cardinali, M., & Reichenbach, P. (1999). Landslide hazard evaluation: a review of current techniques and their application in a multi-scale study, Central Italy. *Geomorphology*, 31(1-4), 181–216. [https://doi.org/10.1016/S0169-555X\(99\)00078-1](https://doi.org/10.1016/S0169-555X(99)00078-1)
- Guzzetti, F., Reichenbach, P., Ardizzone, F., Cardinali, M., & Galli, M. (2006). Estimating the quality of landslide susceptibility models. *Geomorphology*, 81(1-2), 166–184. <https://doi.org/10.1016/j.geomorph.2006.04.007>
- Hadi, A. I., Brotospito, K. S., Pramunijoyo, S., & Hardiatmo, H. C. (2018). Regional Landslide Potential Mapping in Earthquake-Prone Areas of Kepahiang Regency, Bengkulu Province, Indonesia. *Geosciences*, 8(6), 219.
- Hall, F. G., Townshend, J. R., & Engman, E. T. (1995). Status of remote sensing algorithms for estimation of land surface state parameters. *Remote Sensing of Environment*, 51(1), 138–156. [https://doi.org/10.1016/0034-4257\(94\)00071-T](https://doi.org/10.1016/0034-4257(94)00071-T)
- He, H., Hu, D., Sun, O., Zhu, L., & Liu, Y. (2019). A landslide susceptibility assessment method based on GIS technology and an AHP-weighted information content method: A case study of southern Anhui, China. *ISPRS International Journal of Geo-Information*, 8(6), 266. <https://doi.org/10.3390/ijgi8060266>
- Hennrich, K., & Crozier, M. J. (2004). A hillslope hydrology approach for catchment-scale slope stability analysis. *Earth Surface Processes and Landforms: The Journal of the British Geomorphological Research Group*, 29(5), 599–610. <https://doi.org/10.1002/esp.1054>
- Hong, H., Pradhan, B., Xu, C., & Tien Bui, D. (2015). Spatial prediction of landslide hazard at the Yihuang area (China) using two-class kernel logistic regression, alternating decision tree and support vector machines. *Catena* 133, 266–281. <https://doi.org/10.1016/j.catena.2015.05.019>
- Hong, H., Liu, J., Bui, D. T., Pradhan, B., Acharva, T. D., Pham, B. T., & Ahmad, B. B. (2018). Landslide susceptibility mapping using J48 Decision Tree with AdaBoost, Bagging and Rotation Forest ensembles in the Guangchang area (China). *Catena*, 163, 399–413. <https://doi.org/10.1016/j.catena.2018.01.005>
- Huang, Y., & Zhao, L. (2018). Review on landslide susceptibility mapping using support vector machines. *Catena*, 165, 520–529. <https://doi.org/10.1016/j.catena.2018.03.003>
- Ilanloo, M. (2011). A comparative study of fuzzy logic approach for landslide susceptibility mapping using GIS: An experience of Karai dam basin in Iran. *Procedia-Social and Behavioral Sciences*, 19, 668–676. <https://doi.org/10.1016/j.sbspro.2011.05.184>
- Kalantar, B., Pradhan, B., Naghibi, S. A., Motevalli, A., & Mansor, S. (2018). Assessment of the effects of training data selection on the landslide susceptibility mapping: a comparison between support vector machine (SVM), logistic regression (LR) and artificial neural networks (ANN). *Geomatics, Natural Hazards and Risk*, 9(1), 49–69. <https://doi.org/10.1080/19475705.2017.1407368>
- Kanevski, M., Pozdnoukhov, A., & Timonin, V. (2009). Machine learning for spatial environmental data: theory, applications, and software. *EPFL Press, Lausanne*, pp 275. <https://doi.org/10.1201/9781439808085>
- Kanungo, D. P., Arora, M. K., Sarkar, S., & Gupta, R. P. (2006). A comparative study of conventional, ANN black box, fuzzy and combined neural and fuzzy weighting procedures for landslide susceptibility zonation in Darjeeling Himalayas. *Engineering Geology*, 85(3-4), 347–366. <https://doi.org/10.1016/j.enggeo.2006.03.004>
- Kanungo, D.P., Arora, M.K., Sarkar, S., & Gupt, R.P. (2009). Landslide Susceptibility Zonation (LSZ) Mapping - A Review. *Journal of South Asia Disaster Studies, Vol. 2 No. 1*, 81–105.
- Keerthi, S. S., & Lin, C. J. (2003). Asymptotic behaviors of support vector machines with Gaussian kernel. *Neural computation*, 15(7), 1667–1689. <https://doi.org/10.1162/089976603321891855>
- Kornejad, A., Owneh, M., & Bahremand, A. (2017). Landslide susceptibility assessment using maximum entropy model with two different data sampling methods. *Catena*, 152, 144–162. <https://doi.org/10.1016/j.catena.2017.01.010>
- Kuriakose, S. L., Van Beek, L. P. H., & Van Westen, C. J. (2009a). Parameterizing a physically based shallow landslide model in a data poor region. *Earth surface processes and landforms*, 34(6), 867–881. <https://doi.org/10.1002/esp.1794>

- Kuriakose, S. L., Devkota, S., Rossiter, D. G., & Jetten, V. G. (2009b). Prediction of soil depth using environmental variables in an anthropogenic landscape, a case study in the Western Ghats of Kerala, India. *Catena*, 79(1), 27-38. <https://doi.org/10.1016/j.catena.2009.05.005>
- Lacasse, S., & Nadim, F. (2009). Landslide risk assessment and mitigation strategy. In *Landslides–disaster risk reduction* (pp. 31-61). Springer, Berlin, Heidelberg. https://doi.org/10.1007/978-3-540-69970-5_3
- Landis, J. R., & Koch, G. G. (1977). The measurement of observer agreement for categorical data. *biometrics*, 159-174.
- Lee, S., & Min, K. (2001). Statistical analysis of landslide susceptibility at Yongin, Korea. *Environmental geology*, 40(9), 1095-1113. <https://doi.org/10.1007/s002540100310>
- Lee, S., Chwae, U., & Min, K. (2002). Landslide susceptibility mapping by correlation between topography and geological structure: the Janghung area, Korea. *Geomorphology*, 46(3-4), 149-162. [https://doi.org/10.1016/S0169-555X\(02\)00057-0](https://doi.org/10.1016/S0169-555X(02)00057-0)
- Lee, S., Rvu, J.H., Lee, M.J., & Won, J.S. (2003). Use of an artificial neural network for analysis of susceptibility to landslides at Boun, Korea. *Environmental Geology* 34 (1), 59–69. <https://doi.org/10.1007/s00254-003-0825-y>
- Lee, S., & Talib, J. A. (2005). Probabilistic landslide susceptibility and factor effect analysis. *Environmental Geology*, 47(7), 982-990. <https://doi.org/10.1007/s00254-005-1228-z>
- Lee, S., Hwang, J., & Park, I. (2013). Application of data-driven evidential belief functions to landslide susceptibility mapping in Jinbu, Korea. *Catena*, 100, 15-30. <https://doi.org/10.1016/j.catena.2012.07.014>
- Lee, S., Hong, S. M., & Jung, H. S. (2017). A support vector machine for landslide susceptibility mapping in Gangwon Province, Korea. *Sustainability*, 9(1), 48. <https://doi.org/10.3390/su9010048>
- Lin, G. W., Chen, H., Chen, Y. H., & Hornig, M. J. (2008). Influence of typhoons and earthquakes on rainfall-induced landslides and suspended sediments discharge. *Engineering Geology*, 97(1-2), 32–41. <https://doi.org/10.1016/j.enggeo.2007.12.001>
- Lineback, M., Andrew, W., Aspinall, R., & Custer, S. (2001). Assessing landslide potential using GIS, soil wetness modeling, and topographic attributes, Payette River, Idaho. *Geomorphology* 37, 149–165. [https://doi.org/10.1016/S0169-555X\(00\)00068-4](https://doi.org/10.1016/S0169-555X(00)00068-4)
- Marjanović, M., Kovačević, M., Bajat, B., & Voženilek, V. (2011). Landslide susceptibility assessment using SVM machine learning algorithm. *Engineering Geology*, 123(3), 225-234. <https://doi.org/10.1016/j.enggeo.2011.09.006>
- McDermid, G. J., & Franklin, S. E. (1995). Remote sensing and geomorphometric discrimination of slope processes. *Zeitschrift für Geomorphologie. Supplementband*, (101), 165-185.
- Mohammady, M., Pourghasemi, H. R., & Pradhan, B. (2012). Landslide susceptibility mapping at Golestan Province, Iran: a comparison between frequency ratio, Dempster–Shafer, and weights-of-evidence models. *Journal of Asian Earth Sciences*, 61, 221-236. <https://doi.org/10.1016/j.jseas.2012.10.005>
- Moore, I. D., & Burch, G. J. (1986). Sediment transport capacity of sheet and rill flow: application of unit stream power theory. *Water Resources Research*, 22(8), 1350-1360. <https://doi.org/10.1029/WR022i008p01350>
- Moore, I. D., Grayson, R. B., & Ladson, A. R. (1991). Digital terrain modelling: a review of hydrological, geomorphological, and biological applications. *Hydrological processes*, 5(1), 3-30. <https://doi.org/10.1002/hyp.3360050103>
- Nefeslioglu, H. A., Gokceoglu, C., & Sonmez, H. (2008). An assessment on the use of logistic regression and artificial neural networks with different sampling strategies for the preparation of landslide susceptibility maps. *Engineering Geology*, 97(3-4), 171-191. <https://doi.org/10.1016/j.enggeo.2008.01.004>
- Oh, H. J., & Pradhan, B. (2011). Application of a neuro-fuzzy model to landslide-susceptibility mapping for shallow landslides in a tropical hilly area. *Computers & Geosciences*, 37(9), 1264-1276. <https://doi.org/10.1016/j.cageo.2010.10.012>
- Pachauri, A. K., Gupta, P. V., & Chander, R. (1998). Landslide zoning in a part of the Garhwal Himalayas. *Environmental Geology*, 36(3), 325-334. <https://doi.org/10.1007/s002540050348>
- Party, I. L. W. (2007). Iranian landslides list. Forest, Rangeland and Watershed Association: Tehran, Iran, 60.
- Petley, D.N. (2008). The Global Occurrence of Fatal Landslides in 2007, Vol.10. *Geophysical Research Abstracts. EGU General Assembly*, p. 3.
- Pourghasemi, H. R., Pradhan, B., & Gokceoglu, C. (2012a). Application of fuzzy logic and analytical hierarchy process (AHP) to landslide susceptibility mapping at Haraz watershed, Iran. *Natural hazards*, 63(2), 965-996. <https://doi.org/10.1007/s11069-012-0217-2>
- Pourghasemi, H. R., Pradhan, B., Gokceoglu, C., & Moezzi, K. D. (2012b). Landslide susceptibility mapping using a spatial multi criteria evaluation model at Haraz Watershed, Iran. In *Terrigenous mass movements* (pp. 23-49). Springer, Berlin, Heidelberg. https://doi.org/10.1007/978-3-642-25495-6_2

- Pourghasemi, H. R., Moradi, H. R., & Aghda, S. F. (2013a). Landslide susceptibility mapping by binary logistic regression, analytical hierarchy process, and statistical index models and assessment of their performances. *Natural hazards*, 69(1), 749-779. <https://doi.org/10.1007/s11069-013-0728-5>.
- Pourghasemi, H. R., Pradhan, B., Gokceoglu, C., Mohammadi, M., & Moradi, H. R. (2013b). Application of weights-of-evidence and certainty factor models and their comparison in landslide susceptibility mapping at Haraz watershed, Iran. *Arabian Journal of Geosciences*, 6(7), 2351-2365. <https://doi.org/10.1007/s12517-012-0532-7>
- Pourghasemi, H. R., Jirandeh, A. G., Pradhan, B., Xu, C., & Gokceoglu, C. (2013c). Landslide susceptibility mapping using support vector machine and GIS at the Golestan Province, Iran. *Journal of Earth System Science*, 122(2), 349-369. <https://doi.org/10.1007/s12040-013-0282-2>
- Pourghasemi, H.R., & Rahmati, O. (2018). Prediction of the landslide susceptibility: which algorithm, which precision? *Catena* 162, 177–192. <https://doi.org/10.1016/j.catena.2017.11.022>
- Pourghasemi, H. R., Gaven, A., Panahi, M., Rezaie, F., & Blaschke, T. (2019). Multi-hazard probability assessment and mapping in Iran. *Science of the total environment*, 692, 556-571. Error! Hyperlink reference not valid. <https://doi.org/10.1016/j.scitotenv.2019.07.203>
- Pourghasemi, H. R., Kariminejad, N., Amiri, M., Edalat, M., Zarafshar, M., Blaschke, T., & Cerda, A. (2020). Assessing and mapping multi-hazard risk susceptibility using a machine learning technique. *Scientific reports*, 10(1), 1-11. <https://doi.org/10.1038/s41598-020-60191-3>
- Pradhan, B., & Lee, S. (2010). Landslide susceptibility assessment and factor effect analysis: back propagation artificial neural networks and their comparison with frequency ratio and bivariate logistic regression modelling. *Environmental Modelling & Software*, 25(6), 747-759. <https://doi.org/10.1016/j.envsoft.2009.10.016>
- Pradhan, B. (2011). Use of GIS-based fuzzy logic relations and its cross application to produce landslide susceptibility maps in three test areas in Malaysia. *Environmental Earth Sciences*, 63(2), 329-349. <https://doi.org/10.1007/s12665-010-07051>
- Pradhan, B. (2013). A comparative study on the predictive ability of the decision tree, support vector machine and neuro-fuzzy models in landslide susceptibility mapping using GIS. *Computers & Geosciences*, 51, 350-365. <https://doi.org/10.1016/j.cageo.2012.08.023>
- Pradhan, A. M. S., & Kim, Y. T. (2016). Evaluation of a combined spatial multi-criteria evaluation model and deterministic model for landslide susceptibility mapping. *Catena*, 140, 125-139. <https://doi.org/10.1016/j.catena.2016.01.022>
- Reichenbach, P., Rossi, M., Malamud, B. D., Mihir, M., & Guzzetti, F. (2018). A review of statistically-based landslide susceptibility models. *Earth-Science Reviews*, 180, 60-91. <https://doi.org/10.1016/j.earscirev.2018.03.001>
- Roccati, A., Faccini, F., Luino, F., Ciampalini, A., & Turconi, L. (2019). Heavy rainfall triggering shallow landslides: A susceptibility assessment by a GIS-approach in a Ligurian Apennine Catchment (Italy). *Water*, 11(3), 605. <https://doi.org/10.3390/w11030605>
- Saha, A. K., Gupta, R. P., Sarkar, I., Arora, M. K., & Csaplovics, E. (2005). An approach for GIS-based statistical landslide susceptibility zonation—with a case study in the Himalayas. *Landslides*, 2(1), 61-69. <https://doi.org/10.1007/s10346-004-0039-8>
- Shrestha, D. P., & Zinck, J. A. (2001). Land use classification in mountainous areas: integration of image processing, digital elevation data and field knowledge (application to Nepal). *International Journal of Applied Earth Observation and Geoinformation*, 3(1), 78-85. [https://doi.org/10.1016/S0303-2434\(01\)85024-8](https://doi.org/10.1016/S0303-2434(01)85024-8)
- Sidle, R. C., Pearce, A. J., & O'Loughlin, C. L. (1985). *Hillslope stability and land use*. American geophysical union. <https://doi.org/10.1029/WM011>
- Song, S., Zhan, Z., Long, Z., Zhang, J., & Yao, L. (2011). Comparative study of SVM methods combined with voxel selection for object category classification on fMRI data. *PloS one*, 6(2), e17191. <https://doi.org/10.1371/journal.pone.0017191>
- Suzen, M. L., & Toprak, V. E. D. A. T. (1998). Filtering of satellite images in geological lineament analyses: an application to a fault zone in Central Turkey. *International journal of remote sensing*, 19(6), 1101-1114. <https://doi.org/10.1080/014311698215621>
- Talebi, A., Troch, P. A. A., & Uijlenhoet, R. (2006). A steady-state analytical hillslope stability model. <https://doi.org/10.1002/hyp.6881>
- Talebi, A., Uijlenhoet, R., & Troch, P. A. (2008a). A low-dimensional physically based model of hydrologic control of shallow landsliding on complex hillslopes. *Earth Surface Processes and Landforms: The Journal of the British Geomorphological Research Group*, 33(13), 1964-1976. <https://doi.org/10.1002/esp.1648>
- Talebi, A., Uijlenhoet, R., & Troch, P. A. (2008b). Application of a probabilistic model of rainfall-induced shallow landslides to complex hollows. *Natural Hazards and Earth System Sciences*, 8(4), 733-744. <https://doi.org/10.5194/nhess-8-733-2008>
- Tangestani, M. H., & Moore, F. (2001). Porphyry copper potential mapping using the weights of evidence model in a GIS, northern Shahr e Babak, Iran. *Australian Journal of Earth Sciences*, 48(5), 695-701. <https://doi.org/10.1046/j.1440-0952.2001.485889.x>

- Troch, P. A., Paniconi, C., & Emiel van Loon, A. E. (2003). Hillslope-storage Boussinesq model for subsurface flow and variable source areas along complex hillslopes: 1. Formulation and characteristic response. *Water Resources Research*, 39(11). <https://doi.org/10.1029/2002WR001728>
- Tseng, C. M., Lin, C. W., & Hsieh, W. D. (2015). Landslide susceptibility analysis by means of event-based multi-temporal landslide inventories. *Natural Hazards and Earth System Sciences Discussions*, 3(2), 1137-1173. <https://doi.org/10.5194/nhessd-3-1137-2015>
- Van Beek, L. P. H., & Van Asch, T. W. (2004). Regional assessment of the effects of land-use change on landslide hazard by means of physically based modelling. *Natural Hazards*, 31(1), 289-304. <https://doi.org/10.1023/B:NHAZ.0000020267.39691.39>
- Van Beek, L.P.H., Wint, J., Cammeraat, L.H., & Edwards, J.P. (2005). Observation and simulation of root reinforcement on abandoned Mediterranean slopes: Plant and Soil. 278, p. 55-74. <https://doi.org/10.1007/s11104-005-7247-4>
- Van Westen, C. J., & Alzate Bonilla, J. B. (1990). Mountain hazard analysis using a PC-based GIS. In *International congress international association of engineering geology*. 6 (pp. 265-271).
- Van Westen, C. J., Van Asch, T. W., & Soeters, R. (2006). Landslide hazard and risk zonation—why is it still so difficult?. *Bulletin of Engineering geology and the Environment*, 65(2), 167-184. <https://doi.org/10.1007/s10064-005-0023-0>
- Vapnik, V.N. (2001). The nature of statistical learning theory. *Statistics for Engineering and Information Science*, 2nd edn. Springer, New York. <https://doi.org/10.1007/978-1-4757-3264-1>
- Vijith, H., & Madhu, G. (2008). Estimating potential landslide sites of an upland sub-watershed in Western Ghat's of Kerala (India) through frequency ratio and GIS. *Environmental Geology*, 55(7), 1397-1405. <https://doi.org/10.1007/s00254-007-1090-2>
- Wang, C. M., & Huang, Y. F. (2009). Evolutionary-based feature selection approaches with new criteria for data mining: A case study of credit approval data. *Expert systems with Applications*, 36(3), 5900-5908. <https://doi.org/10.1016/j.eswa.2008.07.026>
- Wang, L. J., Sawada, K., & Moriguchi, S. (2013). Landslide susceptibility analysis with logistic regression model based on FCM sampling strategy. *Computers & Geosciences*, 57, 81-92. <https://doi.org/10.1016/j.cageo.2013.04.006>
- Weier, J., & Herring, D. (2005). Measuring vegetation (NDVI and EVI). Earth observatory Library of NASA, <http://earthobservatory.nasa.gov/Library/MeasuringVegetation/>.
- Wischmeier, W. H., & Smith, D. D. (1978). *Predicting rainfall erosion losses: a guide to conservation planning* (No. 537). Department of Agriculture, Science and Education Administration.
- Wu, W., & Sidle, R. C. (1995). A distributed slope stability model for steep forested basins. *Water resources research*, 31(8), 2097-2110. <https://doi.org/10.1029/95WR01136>
- Xiao, T., Yin, K., Yao, T., & Liu, S. (2019). Spatial prediction of landslide susceptibility using GIS-based statistical and machine learning models in Wanzhou County, Three Gorges Reservoir, China. *Acta Geochim.* 38, 654–669. <https://doi.org/10.1007/s11631-019-00341-1>
- Yalcin, A. (2005). An investigation on Ardesen (Rize) region on the basis of landslide susceptibility. Ph.D. Thesis, Karadeniz Technical University, Trabzon, Turkey (in Turkish).
- Yan, F., Zhang, O., Ye, S., & Ren, B. (2019). A novel hybrid approach for landslide susceptibility mapping integrating analytical hierarchy process and normalized frequency ratio methods with the cloud model. *Geomorphology*, 327, 170-187. <https://doi.org/10.1016/j.geomorph.2018.10.024>
- Yao, X., Zhang, Y.S., Wang, X.L., & Xiong, T.Y. (2008). Automatic hierarchical approach to detecting shallow landslides and avalanches by the combination of multi-spectral RS imagery and DEM derivatives. *Geol Bull China* 27:1870–1874.
- Yao, X., Tham, L. G., & Dai, F. C. (2008b). Landslide susceptibility mapping based on support vector machine: a case study on natural slopes of Hong Kong, China. *Geomorphology*, 101(4), 572-582. <https://doi.org/10.1016/j.geomorph.2008.02.011>
- Yeon, Y. K., Han, J. G., & Rvu, K. H. (2010). Landslide susceptibility mapping in Iniae, Korea, using a decision tree. *Engineering Geology*, 116(3-4), 274-283. <https://doi.org/10.1016/j.enggeo.2010.09.009>
- Yilmaz, I. (2009). Landslide susceptibility mapping using frequency ratio, logistic regression, artificial neural networks and their comparison: a case study from Kat landslides (Tokat—Turkey). *Computers & Geosciences*, 35(6), 1125-1138. <https://doi.org/10.1016/j.cageo.2008.08.007>
- Yilmaz, I. (2010). Comparison of landslide susceptibility mapping methodologies for Koyulhisar, Turkey: conditional probability, logistic regression, artificial neural networks, and support vector machine. *Environmental Earth Sciences*, 61(4), 821-836. <https://doi.org/10.1007/s12665-009-0394-9>
- Zare, M., Pourghasemi, H. R., Vafakhah, M., & Pradhan, B. (2013). Landslide susceptibility mapping at Vaz Watershed (Iran) using an artificial neural network model: a comparison between multilayer perceptron (MLP) and radial basic function (RBF) algorithms. *Arabian Journal of Geosciences*, 6(8), 2873-2888. <https://doi.org/10.1007/s12517-012-0610-x>

- Zhao, S., & Zhao, Z. A Comparative Study of Landslide Susceptibility Mapping Using SVM and PSO-SVM Models Based on Grid and Slope Units. *Mathematical Problems in Engineering*, 2021. <https://doi.org/10.1155/2021/8854606>
- Zhu, X., Zhang, S., Jin, Z., Zhang, Z., & Xu, Z. (2010). Missing value estimation for mixed-attribute data sets. *IEEE Transactions on Knowledge and Data Engineering*, 23(1), 110-121. <https://doi.org/10.1109/TKDE.2010.99>



© 2021 by the authors. Licensee IAU, Maybod, Iran. This article is an open access article distributed under the terms and conditions of the Creative Commons Attribution (CC BY) license (<http://creativecommons.org/licenses/by/4.0/>).